ARTICLE

Field Electron Emission Characteristics and Physical Mechanism of Individual Single-Layer Graphene

Zhiming Xiao,[†] Juncong She,[†,*] Shaozhi Deng,[†] Zikang Tang,[†,‡] Zhibing Li,[†] Jianming Lu,[‡] and Ningsheng Xu[†,*]

[†]State Key Lab of Optoelectronic Materials and Technologies and Guangdong Province Key Laboratory of Display Material and Technology, School of Physics and Engineering, Sun Yat-sen University, Guangzhou 510275, People's Republic of China, and [‡]Department of Physics, Hong Kong University of Science and Technology, Clear Water Bay, Kowloon, Hong Kong, People's Republic of China

ABSTRACT Due to its difficulty, experimental measurement of field emission from a single-layer graphene has not been reported, although field emission from a two-dimensional (2D) regime has been an attractive topic. The open surface and sharp edge of graphene are beneficial for field electron emission. A 2D geometrical effect, such as massless Dirac fermion, can lead to new mechanisms in field emission. Here, we report our findings from *in situ* field electron emission characterization on an individual singe-layer graphene and the understanding of the related mechanism. The measurement of field emission from the edges was done using a microanode probe equipped in a scanning electron microscope. We show that repeatable stable field emission current can be obtained after a careful conditioning process. This enables us to examine experimentally the typical features of the field emission from a 2D regime. We plot current versus applied field data, respectively, in $\ln(I/E^{3/2}) \sim 1/E$ and $\ln(I/E^{3}) \sim 1/E^{2}$ coordinates, which have recently been proposed for field emission from graphene in high- and low-field regimes. It is observed that the plots all exhibit an upward bending feature, revealing that the field emission processes undergo from a low- to high-field transition. We discuss with theoretical analysis the physical mechanism responsible for the new phenomena.

KEYWORDS: field emission · single-layer graphene · microanode probe · upward bending FN plot · 2D regime · line current density

*Address correspondence to stsxns@mail.sysu.edu.cn, shejc@mail.sysu.edu.cn.

Received for review July 21, 2010 and accepted September 30, 2010.

Published online October 7, 2010. 10.1021/nn101719r

Graphene has an inherent two-dimensional (2D) geometry, open surface and edge. The large aspect ratio due to the sharp edge of graphene makes it attractive for field electron emission. More important, field emission from a 2D regime has not been studied. Graphene can offer one such an opportunity. Theory has predicted an unconventional electronic structure of the edge states in graphene,[1] which may affect electron tunneling probability from the edge. Considering massless Dirac fermions in graphene,[2] which have a linear dispersion relation that is different from the quadratic relation of the nonrelativity electrons, the density of states is affected. Thus, further studies are needed on its field emission mechanism. A number of studies have already been carried out on the field emission properties of graphene thin film.[3−5] S. Wang *et al.* studied the high field emission reproducibility and stability of carbon nanosheets.[3] G. Eda and coworkers investigated the field emission from graphene-based composite thin films.[4] They reported the effect of graphene alignment on field emission. Z. S. Wu *et al.* measured the field emission of the films of single-layer graphene.[5] These reports show attractive field emission performance of graphene films, but they represent the collective behavior of a large number of graphenes. To understand the physical mechanism underlying, it is essential to study field emission from a single-layer graphene.

RESULTS AND DISCUSSION

To realize an individual graphene sheet for field emission study, a single graphene sheet was prepared by mechanical cleavage. They were then placed on the surface of the SiO_2 layer that was already prepared by thermally oxidizing a single crystal Si wafer. The thickness of SiO_2 was carefully chosen to ~300 nm to make the single-layer graphene visible under optical microscope. Gold electrodes were deposited on two ends of a single-layer graphene. Optical image of a single-layer graphene and a Raman spectra were taken to confirm that the graphene sample was a single layer. Figure 1 shows the typical Raman spectra and the scanning electron microscopy (SEM) image of the single-layer graphene.

The field emission measurement was performed in a SEM chamber equipped with a nanomanipulator,[6] which was fixed with a cleaned tungsten microtip as the anode probe. Figure 2a shows the SEM image of the test structure. The distance between the anode probe and the graphene was set

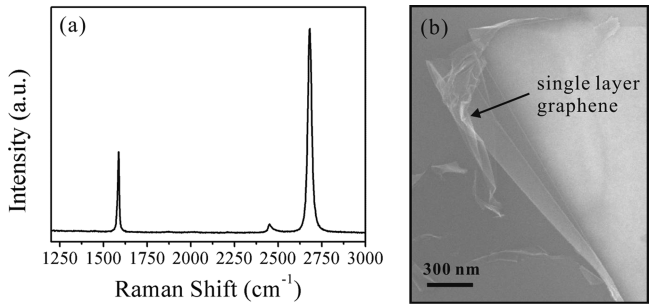

Figure 1. (a) Typical Raman spectrum and (b) SEM image of the single-layer graphenes.

to ~600 nm; at such a small vacuum gap, field enhancement is negligible. We could not succeed in obtaining stable emission when the single layer of graphene laid flat on the substrate. We then used the anode probe to squeeze part of the graphene single layer (as shown in the red dashed square in Figure 2 a, so that it became curled up, as shown by the SEM images in Figure 2b and c. Field emission measurements were performed point by point on the graphene single layer, marked as A−E in Figure 2c and d. With reference to Figure 2d, three types of test points were chosen in our experiment: point A at the edge lying flat on the substrate, point E at the center of the graphene single layer, and points B−D at the edge above the substrate. Only negligible currents with a noise level of <2 pA were observed for points A and E even when the applied electric field was increased to ~800 MV/m. However, field emission currents above 100 pA were observed from points B−D with fields even below 800 MV/m. These reveal that the edge of a single-layer graphene is prone to field electron emission. In order to avoid vacuum breakdown of graphene, the current levels were kept to several hundreds of pico-amperes during our measurements on points B−D.

Typical findings are reported below. First, a room temperature conditioning process can result in a reproducible stable field emission from the edges of a graphene single layer. Such a procedure is described below. The anode voltage was applied on the edge of graphene single layer and increased manually at a voltage step of 0.1 V, and the current was very unstable (Figure 3a). One may see a general trend from Figure 3b that as the number of cycles of voltage increases, gradually a lower voltage (and fields) is needed to obtain the same level of field emission currents. This is completely different from carbon nanotubes, which will emit electrons at much lower fields before conditioning. Also from Figure 3b, currents become more and more stable as the conditioning process goes on. In order to avoid vacuum breakdown, we kept the upper current limit to around 100 pA when the current was seen to be more stable. We finally reach the stage when all *I*−*V* curves are within a narrow range, as may be seen from Figure 3 b (curves 36−49). We enlarged these *I*−*V* curves and show them in Figure 3c. One may see that the fluctuation of current becomes small. This indicates that the edges of the graphene single layer became gradually clean. The small variation in current between the individual voltage cycles may be attributed to other factors, such as mechanical vibration, rather than surface absorption.

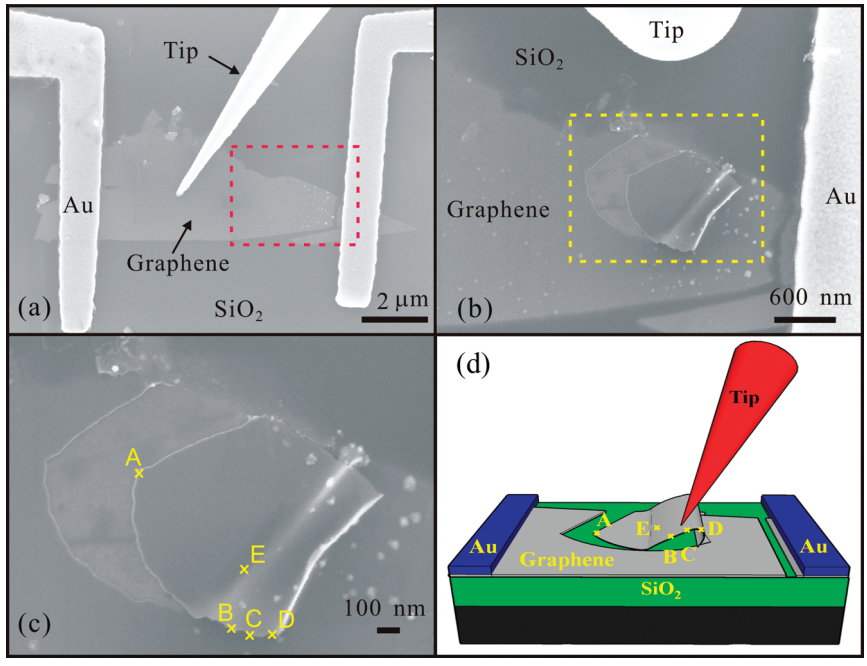

Figure 2. (a) SEM image of the graphene structure and the anode tip for the field emission test. (b) SEM image of the curved graphene, which is located in the red dashed square in (a). (c) Magnified SEM image of the curved graphene in (b). Field emission tests were performed on points A−E. (d) A 3D schematic illustration shows the relative position among anode probe, graphene, test points, and substrate.

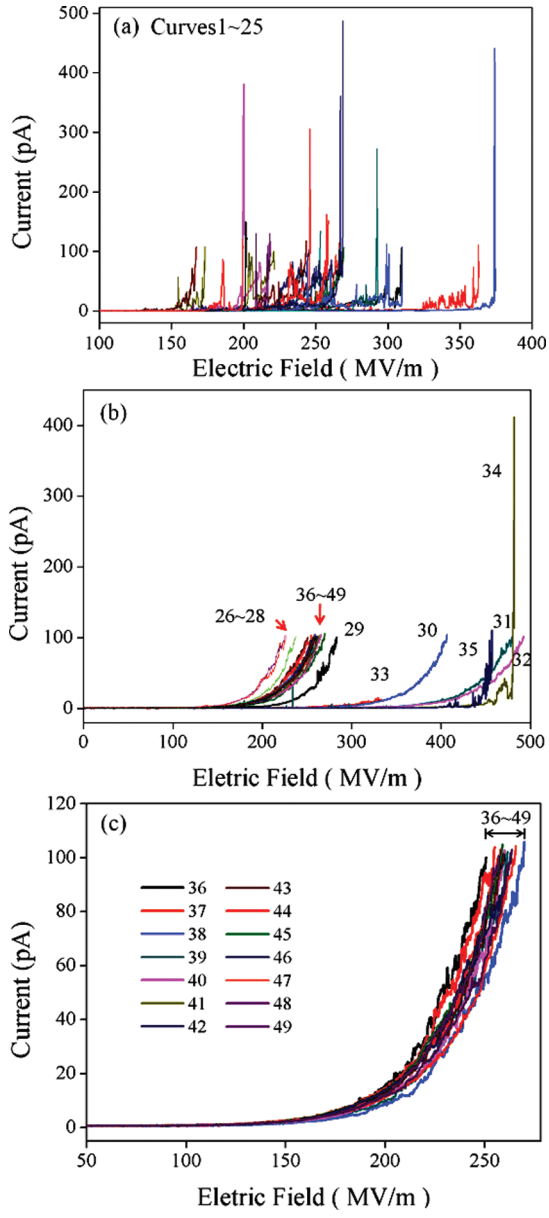

Figure 3. (a) Field emission *I*−*E* curves showing the carefully conditioning processes for continuous testing cycles of 1−25. (b) Curves 26−35 showing the end of the conditioning process before stable and repeatable *I*−*E* curves (36−49) are obtained. (c) Showing stable and repeatable *I*−*E* characteristics obtained after the conditioning.

One can imagine that carbon atoms in the emitting location may also have vibration in such 2D field emission regimes, and in the present study, we have not been able to characterize this effect on electron emission.

In order to find the physical mechanism underlying, it is essential to further analyze the field emission *I*−*V* data. Early reports gave Fowler−Nordheim (FN) plots[3−5] by assuming that the field emission from graphene films may follow the prediction of the conventional FN equation. However, here we are dealing with field emission from single-layer graphene, which is a 2D regime, so we should take the effect of the 2D system into account. Recently, we have derived an analytical solution of the line current density (LCD) of field emission from the nanosheet,[7] which takes into account the effect of quantization of the motion in the direction perpendicular to the sheet. The zero-field barrier height seen by an electron in a state with a transversal kinetic energy $W_\perp$ is $\phi_s = \phi + W_\perp + W_s$,[7,8] with ϕ the work function of the material and W_s the energy difference between the Fermi level and the state. This effect makes the longitudinal energy of electron significantly small, so that when the surface barrier is large, the probability of electron tunneling through the barrier becomes small. Only states close to the state whose surface barrier is relatively small can have contribution to the emission. But the above model should be developed to take into account the physical property of graphene. For graphene, first, the external applied field may penetrate into it, and it leads to induced charges accumulating near the emitting edge. Also, the K state (Dirac point) has the minimum surface barrier, $\phi_K \sim \phi$ (work function $\phi = 4.7$ eV). The state corresponding to the next smallest surface barrier minimum is the M state, and $\phi_M \sim \phi + |t| \sim 7.4$ eV, with t being the hopping parameter of graphene. So the K-state emission is dominated, thus here after only the K-state emission is considered.

The solution for the emission line current density may be expressed below:

$$I(E) = z^{nw} d_E^{3/2} \exp\left(-\frac{b}{\Gamma_E}\frac{\varphi_K^{3/2}}{E}\right) \quad (1)$$

where z^{nw} is a positive constant, which is irrelevant to our discussion, and $b = 6.83\ \mathrm{eV}^{-3/2}\ \mathrm{V\ nm}^{-1}$. The parameters d_E and Γ_E may depend on the applied field E, and they are related to each other *via*[9]

$$d_E^{-1} = \frac{b}{E}\frac{\partial}{\partial\varphi_K}\left(\frac{\varphi_K^{3/2}}{\Gamma_E}\right) \quad (2)$$

The power 3/2 of d_E in eq 1 originates from the 2D supply function.

In the following, we look into both high- and low-field cases. In the high-field regime, the barrier thickness is very small, therefore electrons having longitudinal energies significantly smaller than the Fermi energy may tunnel through the barrier. As a result of the small barrier thickness, the effect of the surface barrier modification due to the specific geometry of the edge of graphene and the distribution of the induced charge is not significant.[7] The triangular barrier is then a good approximation for the surface barrier. Then Γ_E is reduced to the field enhancement factor (γ), and eq 1 becomes

$$I_H(E) \sim E^{3/2} \exp\left(-\frac{b\varphi_K^{3/2}}{\gamma E}\right) \quad (3)$$

In eq 3 there are two notable features that are different from the conventional FN theory for the 3D

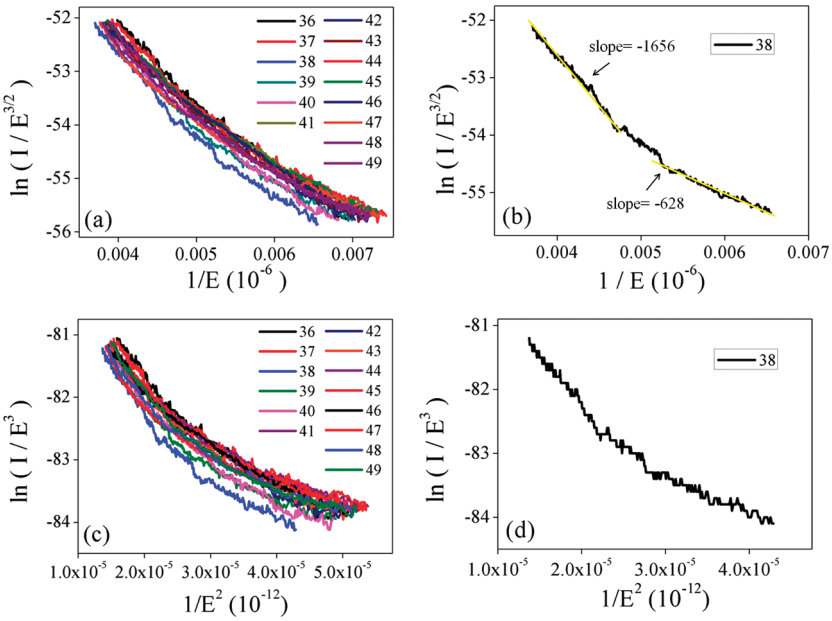

Figure 4. (a) Curves in ln($I/E^{3/2}$) ~ 1/E coordinate, and (b) Single curve for clear exhibition of the upward bending feature. The units of I and E are ampere (A) and volt/meter (V/m), respectively. The inset numbers in (b) are the slope values of the fitting straight lines, while (c) and (d) show the curves in the ln(I/E^3) ~ 1/E^2 coordinate. All the curves in this figure correspond to all the $I-E$ curves 36−49 shown in Figure 3c.

system: (1) The power of E in the prefactor is 3/2 instead of 2 in the FN theory, and (2) The work function of the FN theory is replaced by ϕ_K, the zero-field barrier height seen by an electron in the K state.

Next, when the field on the edge of graphene is weak, the graphene can screen the field almost completely and may be considered as an ideal metallic sheet of zero thickness. As an approximation, we assume that the induced charge is located along a line at distance r from the edge, with r being the field penetration depth. Further, let the line density of the induced charge be λ. One can find that $\Gamma_E = \gamma + \lambda(2\pi\varepsilon_0 rE)^{-1} \approx \lambda(2\pi\varepsilon_0 rE)^{-1}$. In the last step, we have used the fact that the surface barrier is mainly determined by the induced charge in the weak-field regime. It is known that the density of state is linear in the vicinity of the K point, therefore, $\lambda \sim \mu|\mu|$, with the μ being the chemical potential relative to the energy of the K state. It is reasonable to assume that μ is proportional to the edge field as γE. With all of these arguments we obtain the weak-field parameter $\Gamma_E = \kappa\gamma^2 E$, where the parameter κ depends on r and the graphene band structure [using the tight-binding band structure of the graphene, $\kappa \sim 3e^3r^2/(16\pi^2\varepsilon_0 a^2t^2)$]. This is consistent with the sophisticated solution for the flat sheet.[7] Finally, the LCD in the low-field regime follows

$$I_W(E) \sim E^3 \exp\left(-\frac{b\varphi_K^{3/2}}{\kappa\gamma^2 E^2}\right) \quad (4)$$

Now we can plot the $I-E$ data in coordinates: ln(I/E^α) ~ 1/E^β. When (α, β) = (3/2, 1), we have plots as shown in Figure 4a and b, which should be straight lines in the high-field region as predicted by eq 3. When (α, β) = (3, 2), we have plots as shown in Figure 4c and d, which should be straight lines in the low-field region as predicted by eq 4. We can see that, in fact, the curves in all cases exhibit an up-bending feature but no linearity. This up-bending feature is very unique to single-layer graphene and was not reported in the early studies.[3−5] It reveals that as field increases, the emission efficiency becomes higher and higher, as compared to the nonlinear FN plot often reported of carbon nanotubes, nanowires, and diamond and related films, where it shows down bending with increase of the field. In those cases, as the field increases, the field emission gradually emerges into a current saturation region.

More important, this up-bending feature reveals that only eqs 3 or 4 are not enough to explain our experimental findings. We shall demonstrate in the following that both equations are needed because the field emission process we measured involves the underlying physics predicted by the two equations.

Let us compare the slops of the plot ln(I/E^α) ~ 1/E^β in the high- and low-field regimes. Denote the high- and low-field are E_H and E_W, respectively. From eqs 3 and 4, ignoring the prefactors, the slop difference between the high- and the low-field parts of a curve, *i.e.*, the high- minus low-field slop may be written as

$$\Delta_1 = -\frac{b\varphi_K^{3/2}}{\gamma}\left(1 - \frac{2}{\kappa\gamma E_W}\right) \quad (5)$$

for $\beta = 1$, and

$$\Delta_2 = -\frac{b\varphi_K^{3/2}E_H}{2\gamma}\left(1 - \frac{2}{\kappa\gamma E_H}\right) \quad (6)$$

for $\beta = 2$. When $\Delta_1 < 0$, the plot in the coordinates with $\beta = 1$ will bend upward. Using the graphene parameters, we estimate $\kappa = 0.78r^2/(nm \cdot V)$. Therefore, the up-bending condition for the $\beta = 1$ plot is fulfilled when $\gamma E_W r^2 > 2.56V \cdot nm^2$. When $\gamma r^2 > 14.2$ nm^2, the field derived will be within the range of our experimental applied field. The valid regime is even wider if the penetration depth is larger. Since $E_H > E_W$ by definition, whenever those of $\beta = 1$ are bending up, *i.e.*, $\Delta_1 < 0$, one has $\Delta_2 < 0$, thereby the plot with $\beta = 2$ must also bend upward and more obviously than the plot of $\beta = 1$. It is indeed what we observed in Figure 4. Let us consider Figure 4b, the slop difference between high- and low-field regimes is about 1 V/nm (1000 V/μm) that coincides with $-\Delta_1$ given by eq 5 if $\gamma = 5$ and $r = 3.9$ nm.

We may also consider another effect of applied electric field that can lead to gradually increase the electron supply to field emission. It is reported[10,11] that in a field effect transistor (FET) device structure, when applying a field to a graphene single layer, its conductivity (σ) will increase. In our field emission regime, electric fields are constantly applied on the graphene and gradually increase. Thus, the supply of electrons to the emitting edge of the graphene will be strongly affected by the applied electric field. According to the above discussion, using findings reported by A. Barreiro *et al.*[10] and I. Meric *et al.*,[11] one can reason that with increasing the applied electric field in the field emission experiment, the current flows from the substrate to the emitting edge of graphene tend to increase. This can also explain why the FN curves bend upward. More studies are needed to find out the correlation.

CONCLUSIONS

Field emission from a cleaned single-layer graphene can be obtained following a conditioning procedure. Theoretical $I-E$ equations are derived specifically for single-layer graphene and are different from the conventional FN equation. More specific equations for high- and low-field cases are obtained as $\ln(I/E^{\alpha}) \sim 1/E^{\beta}$, where $(\alpha, \beta) = (3/2, 1)$ for the high-field regime and $(\alpha, \beta) = (3, 2)$ for the low-field regime. These are applied successfully to analyze experimental data obtained in this study. All the resultant plots of $\ln(I/E^{\alpha}) \sim 1/E^{\beta}$ exhibit an up-bending feature, showing that field emission from a single-layer graphene can be more and more efficient as the applied field increases. Also, the up-bending feature indicates that the field emission processes can undergo a low- to high-field transition. These findings enhance the knowledge of field emissions from a two-dimension system.

METHODS

A single graphene sheet was prepared by mechanical cleavage. They were placed on silicon substrate with a SiO_2 layer (300 nm in thickness) to make the single-layer graphene, visible under optical microscope. Optical image of a single-layer graphene and Raman spectra was taken to confirm that the graphene sample was a single layer. Gold electrodes were fabricated on the two ends of a single-layer graphene using e-beam lithography, sputtering deposition of Au and PMMA lift-off process.

The field emission measurement on single-layer graphene was performed in a SEM chamber equipped with a nanomanipulator, which was fixed with a cleaned tungsten tip with a radius of 800 nm as the anode probe. In the experiments, the distance between the anode probe and the graphene was set to ~600 nm. A picoammeter with a power supply (Keithley 6487) was employed to record the field emission current. The typical vacuum chamber pressure was $\sim 8 \times 10^{-5}$ Pa.

Acknowledgment. The authors gratefully acknowledge the financial support of the projects from the National Natural Science Foundation of China (grant nos. U0634002, 50725206, 60771055, and 50972168), the National Basic Research Program of China (grant nos. 2010CB327703 and 2007CB935501), the Science and Technology Department of Guangdong Province, the Economic and Information Industry Commission of Guangdong Province, and the Science and Technology and Information Department of Guangzhou City. J.S. is also thankful for the support of the projects from FANEDD (grant no. 200927) and Sun Yat-sen University.

Supporting Information Available: Theoretical model for κ. This material is available free of charge *via* the Internet at http://pubs.acs.org.

REFERENCES AND NOTES

1. Nakada, K.; Fujita, M.; Dresselhaus, G.; Dresselhaus, M. S. Edge State in Graphene Ribbons: Nanometer Size Effect and Edge Shape Dependence. *Phys. Rev. B: Condens. Matter Mater. Phys.* **1996**, *54*, 17954–17961.
2. Novoselov, K. S.; Geim, A. K.; Morozov, S. V.; Jiang, D.; Zhang, Y.; Dubonos, S. V.; Grigorieva, I. V.; Firsov, A. A. Electric Field Effect in Atomically Thin Carbon Films. *Science* **2004**, *306*, 666–669.
3. Wang, S.; Wang, J. J.; Miraldo, P.; Zhu, M. Y.; Outlaw, R.; Hou, K.; Zhao, X.; Holloway, B. C.; Manos, D. High Field Emission Reproducibility and Stability of Carbon Nanosheets and Nanosheet-Based Backgated Triode Emission Devices. *Appl. Phys. Lett.* **2006**, *89*, 183103.
4. Eda, G.; Unalan, H. E.; Rupesinghe, N.; Amaratunga, G. A. J.; Chhowalla, M. Field Emission from Graphene Based Composite Thin Films. *Appl. Phys. Lett.* **2008**, *93*, 233502.
5. Wu, Z. S.; Pei, S. F.; Ren, W. C.; Tang, D. M.; Gao, L. B.; Liu, B. L.; Li, F.; Liu, C.; Cheng, H. M. Field Emission of Single-Layer Graphene Films Prepared by Electrophoretic Deposition. *Adv. Mater.* **2009**, *21*, 1756–1760.
6. Xiao, Z. M.; She, J. C.; Li, Z. B.; Yang, Y. H.; Yang, G. W.; Deng, S. Z.; Chen, J.; Xu, N. S. Oscillating Current Observed in Field Emission from A Single Zinc Oxide Nanostructure and the Physical Mechanism. *J. Appl. Phys.* **2009**, *106*, 014310.
7. Qin, X. Z.; Wang, W. L.; Xu, N. S.; Li, Z. B.; Forbes, R. G. Analytical Solution for Cold Field Electron Emission from A Nanowall Emitter, *Proc. Roc. Soc.* doi:10.1098/rspa.2010.0460.
8. Edgcombe, C. J. New Dimensions for Field Emission: Effects of Structure in the Emitting Surface. *Adv. Imaging Electron Phys.* **2010**, *162*, 77–127.
9. Gadzuk, J. W.; Plummer, E. W. Field Emission Energy Distribution (FEED). *Rev. Mod. Phys.* **1973**, *45*, 487–598.
10. Barreiro, A.; Lazzeri, M.; Moser, J.; Mauri, F.; Bachtold, A. Transport Properties of Graphene in the High-Current Limit. *Phys. Rev. Lett.* **2009**, *103*, 076601.
11. Meric, I.; Han, M. Y.; Young, A. F.; Ozyilmaz, B.; Kim, P.; Shepard, K. L. Current Saturation in Zero-Bandgap, Topgated Graphene Field-Effect Transistors. *Nat. Nanotechnol.* **2008**, *3*, 654–659.